Room temperature line lists for deuterated water

Aleksandra A. Kyuberis [a], Nikolay F. Zobov [a], Olga V. Naumenko [b], Boris A. Voronin [b], Oleg L. Polyansky [c,a], Lorenzo Lodi [c], Anwen Liu [d], Shui-Ming Hu [d], Jonathan Tennyson [c,*]

[a] Institute of Applied Physics, Russian Academy of Sciences, Ulyanov Street 46, Nizhny Novgorod 603950, Russia
[b] V.E. Zuev Institute of Atmospheric Optics, SB RAS, 1, Academician Zuev Square, Tomsk 634021, Russia
[c] Department of Physics and Astronomy, University College London, London, WC1E 6BT, UK
[d] Hefei National Laboratory for Physical Sciences at Microscale, Department of Chemical Physics, University of Science and Technology of China, Hefei 230026, China

ARTICLE INFO

ABSTRACT

Line lists are presented for six deuterated isotopologues of water vapor namely $HD^{16}O$, $HD^{17}O$, $HD^{18}O$, $D_2^{16}O$, $D_2^{17}O$ and $D_2^{18}O$. These line lists are prepared using empirically-determined energy levels, where available, to provide transition frequencies and high-quality *ab initio* dipole moment surfaces to provide transition intensities. The reliability of the predicted intensities is tested by computing multiple line lists and analyzing the stability of the results. The resulting intensities are expected to be accurate to a few percent for well-behaved, stable transitions. Complete $T = 296$ K line lists are provided for each species.

1. Introduction

Deuterated water makes a small, but not insignificant, contribution to the absorption of light by water in the Earth's atmosphere. In particular deuteration leads to large shifts in transition frequencies and therefore absorption by deuterated water often occurs in what are known as the water windows due to the absence of absorption by H_2O. In addition HDO spectra have long been used on both the Earth [1–9] and other planets [10,11] as a means to understand their climatic evolution. The increased relative abundance of deuterium on Venus leads to particularly strong HDO spectra [12]. HDO is also well known in cometary spectra [13,14].

Remote sensing of species such as deuterated water relies on access to comprehensive and reliable spectroscopic data. The 2012 release of HITRAN [15] contains partial line lists for ^{16}O, ^{17}O and ^{18}O isotopologues of HDO but, as shown below, these lists all contain significant omissions. The situation with the recent release of GEISA is similarly deficient for $HD^{17}O$ and $HD^{18}O$ [16], but made extensive use of the recent dataset due to Mikhailenko et al. [17] with which we compare below.

D_2O is only present in trace quantities in the earth's atmosphere and, up until now, has not been included in HITRAN. However, the increased abundance of deuterium in planetary atmospheres such as that of Venus means that the abundance of D_2O should also be enhanced. Enhanced D_2O has already been observed in the inner-region of low-mass protostars [18] and in the interstellar medium [19]. Recently D_2O has also been detected in comets [20].

Besides data stored in HITRAN and GEISA mentioned above, there are a number of other, more extensive line lists available for HDO [21,22], D_2O [23,24] or both [25,26]. However none of these line lists have the accuracy generally expected of spectroscopic databases. This work presents new line lists for six isotopologues of water, namely $HD^{16}O$, $HD^{17}O$, $HD^{18}O$, $D_2^{16}O$, $D_2^{17}O$ and $D_2^{18}O$, which are designed to have the accuracy obtained in high resolution spectroscopy experiments. These line lists combine the empirical energy levels derived by a recent IUPAC-sponsored task group [27–31], with accurate *ab initio* transition intensities. The approach employed relies heavily on the work of Lodi and Tennyson [32] whose $H_2^{17}O$ and $H_2^{18}O$ line lists built in this fashion were adopted in the 2012 update of HITRAN and have subsequently been validated in experimental studies [33]; see also the discussion in this issue by Birk et al. [34]. The aim of the present work is to present comprehensive line lists suitable for inclusion in spectroscopic data bases. We note that a similar parallel effort has been conducted for CO_2 [35] and its various isotopologues [36,37].

To ensure the best possible frequency predictions we have updated the IUPAC lists of empirical energy levels using up-to-date experimental sources. In particular, for the $HD^{17}O$, $HD^{18}O$, $D_2^{17}O$ and $D_2^{18}O$ line lists we have taken advantage of very recent experimental data recorded at the University of Science and Technology of China, Hefei. These experiments are described in Section 3, after we give the theoretical methodology. Results are presented in Section 4 with our final, recommended line lists for each isotopologue given in the supplementary material.

* Corresponding author.
E-mail address: j.tennyson@ucl.ac.uk (J. Tennyson).

2. Method

The absorption intensity of a transition, in units of cm/molecule, is given by the expression [38]

$$I_{if} = 4.162034 \times 10^{-19} \, \omega_{if} g_i Q^{-1}(T)$$
$$\times \left[\exp\left(\frac{-c_2 E_i}{T} \right) - \exp\left(\frac{-c_2 E_f}{T} \right) \right] \left| \sum_\alpha \langle i | \mu_\alpha | f \rangle \right|^2 \quad (1)$$

where T is the temperature, c_2 is the second radiation constant, $\omega_{if} = E_f - E_i$ is the transition frequency between the ith and fth state (all in cm^{-1}), and g_i is the total degeneracy factor. $Q(T)$ is the partition function and the final sum represents the linestrength. To calculate the linestrength requires the initial, $|i\rangle$ and final, $|f\rangle$ rotation-vibration wave functions as well the dipole moment surfaces (DMS), μ_α, for each component of the dipole. For water, the DMS comprise a two-dimensional vector since there is no component of the dipole perpendicular to the plane of the molecule. Eq. (1) does not contain a factor for isotopic abundance. Below all results are presented assuming unit abundance of the given isotopologue, unless otherwise stated in which case HITRAN abundances are employed.

To compute accurate rotation-vibration (RV) transition intensities therefore requires a high accuracy DMS and accurate nuclear motion wave functions. Here we use the accurate *ab initio* DMS of Lodi et al. [39] as represented by two separate fits: the most complete fit LTP2011 and a fit with a reduced number of constants, LTP2011S, which is used to check for problems due to over-fitting [40,41]. Since the non-Born-Oppenheimer correction to the DMS for water is known to be small [42,43], the DMS used here was computed assuming the Born-Oppenheimer approximation [39]. This means that the DMS should be equally valid for all isotopologues of water.

Wave functions and corresponding linestrengths were generated using the discrete variable representation (DVR) program suite DVR3D [44]. DVR3D uses an exact representation of the nuclear motion kinetic energy operator so that, within constraints of the Born-Oppenheimer approximation, any uncertainty in the wave functions is due to the potential energy surface (PES) used. As discussed below, two appropriate PES are employed for each system. In principle DVR3D also yields the upper and lower energy levels and hence the transition frequency for each transition. However, these are more accurately determined experimentally and so empirical data [27–31], expanded by inclusion of the newly reported energy levels (see below), are used where ever possible.

At high accuracy, the uncertainty in the linestrength and hence the transition intensity is dominated by the quality of the DMS. However, experience shows that the wave functions can become poorly determined in the region of accidental resonances between nearby states of the same symmetry. In this situation the computed intensity, particularly of weak transitions, can be very sensitive to precise wave functions used and hence can depend strongly on the underlying PES. For this reason the Lodi-Tennyson procedure [32] involves computing four line lists using all combinations of two distinct PES and two DMS. A scatter factor, ρ, is obtained for each transition as the ratio between the strongest and weakest transition intensity. In the absence of any resonance interactions these scatter factors are close to unity. They become large in the region of a resonance, see Ref. [35] for an illustration of this. Transitions with a large scatter factor have intensities not well-determined by our theoretical procedure and their intensities should either be determined by alternative means or given a large uncertainty.

2.1. HD^{16}O

The most abundant deuterated water species is HD^{16}O so this isotopologue required the most extensive variational calculations. In initial studies on HD^{16}O [45], we used a fitted PES [46] and a high-quality *ab initio* one [47]. However this combination was found to give far too many (false) positives in identifying lines with unstable intensities. It was decided that the two PESs were simply too different from each other to be useful for this analysis; it was therefore necessary to compute new line lists based on improved PESs. A similar conclusion was drawn for the studies on CO$_2$, another molecule with a lot of resonances, by Zak et al. [35].

The base potential was the fitted HDO07 PES due to Yurchenko et al. [46]. However, to allow for higher lying levels this potential was adapted by combining with a less accurate, global PES. To do this we adopted a switching function of the form advocated by Varandas [48].

$$V_{\text{global}} = V_{\text{low}} f(E) + V_{\text{up}}(1 - f(E)). \quad (2)$$

The function $f(E)$ changes monotonically from 1 to 0 around 25,000 cm^{-1} over a region of about 1000 cm^{-1}. V_{low} was the spectroscopically-determined PES of Yurchenko et al. [46]; for V_{up} we used a (less accurate) spectroscopically-determined PES constructed to treat highly excited states of HD^{16}O up to 40 000 cm^{-1} using still to be published data from Boyarkin et al.[49]. Lower weights were used for the fit for levels between 25000 and 40,000 cm^{-1}.

Using a purely *ab initio* surface for the second PES gave results which are two far away from the true answers (M.J. Downs, unpublished 2013). We therefore constructed a new global spectroscopically-determined PES by fitting to a combination of the IUPAC empirical energy levels augmented by the new states mentioned above. This potential is also in the form of Eq. (2). The V_{low} in this PES reproduced the observed energy levels 50% less accurately than the PES of Yurchenko et al. [46] making it highly suitable for use in a Lodi-Tennyson stability analysis.

Nuclear motion calculations were performed in Radau coordinates with 30 Gauss–Laguerre DVR points in each radial coordinate and 48 (associated)-Gauss- Legendre points in the angular coordinate. Basis set parameters were taken from Yurchenko et al. [46]. For each rotational state J, two Hamiltonian matrices were diagonalized of dimension $1000 \times (J + 1)$ and $1000 \times J$, depending on their overall parity. Calculations were performed for J up to 23 but we limited our consideration of intensities to transitions below 20 000 cm^{-1} as our available DMS is not good enough to improve on the measured intensities at the highest frequencies [50].

2.2. HD^{17}O and HD^{18}O

Isotopic abundance factors mean that only strong lines belonging to HD^{17}O and HD^{18}O are important for atmospheric studies. This raises less issues with unstable intensities. For these species line lists generated by Down [45] were used. These line lists used the HD^{16}O fitted PES [46] as their basis and the high-quality *ab initio* CVRQD PES [47] for the second potential. Further details can be found in Down's PhD thesis [45].

2.3. D$_2$O

For D$_2$O the base PES was that of Shirin et al. [24] which was explicitly developed for D$_2$O. This PES gives high accuracy results: our calculations found that it reproduced the empirical levels below 15,000 cm^{-1} with $J \leq 10$ with an rms of 0.023 cm^{-1}. Again a two term PES in the form of Eq. (2) was used with V_{up} taken from a

Table 1
Summary of new line lists in comparison with data in HITRAN 2012 [15]; N is the number of transitions contained in each list.

isotopologue	HITRAN 2012		This work	
	coverage (cm^{-1})	N	coverage (cm^{-1})	N
HD^{16}O	0–22,708	13237	0–19936	56430
HD^{18}O	0–3825	1611	0–12000	10664
HD^{17}O	1234–1599	175	0–10703	6366
D$_2^{16}$O	–	0	0–12797	23195
D$_2^{18}$O	–	0	0–5455	3823
D$_2^{17}$O	–	0	0–5455	2202

recent study on H$_2^{16}$O [51]. For the second PES we used a fitted (to H$_2^{16}$O data) mass-independent (Born–Oppenheimer) PES plus adiabatic and non-adiabatic corrections [51]. This PES reproduced the same basket of empirical levels with an rms of 0.05 cm^{-1}.

For D$_2^{16}$O transition frequencies up to about 25,000 cm^{-1} for J up to 20 were considered. DVR3D calculations in Radau co-ordinates used 29 radial grid points and 40 angular grid points. Vibrational Hamiltonian matrices of final dimension 1500 were diagonalized and for the full rotation-vibration Hamiltonian the matrices had dimension $300 \times (J + 1)$ and $300 \times J$. D$_2^{16}$O showed rather few unstable lines.

As only very strong lines are needed for D$_2^{17}$O and D$_2^{18}$O, a single line list was computed. This line list is based on the D$_2$O PES of Shirin et al. [24] and the LTP2011 DMS. Only J's up to 15 were considered, otherwise the other DVR3D parameters were the same as for D$_2^{16}$O.

3. New experimental data

Fourier transform spectra of the deuterated water enriched by ^{18}O were recorded between 2088 and 6300 cm^{-1} in Hefei. The spectra were measured with the Fourier-transform spectrometer (Bruker IFS 120 HR) equipped with a path length adjustable multi-pass cell. The experimental conditions in the different regions have been listed in Table 1 of Ref [52]. The line positions were calibrated using absorption lines of H$_2^{16}$O and HD^{16}O taken from the HITRAN 2012 database. The accuracy of the line positions of unblended and not-very-weak lines was estimated to be better than 0.0004 cm^{-1}.

The observed spectrum comprises transitions attributed to nine water isotopologues: H$_2^{16}$O, H$_2^{18}$O, H$_2^{17}$O, HD^{16}O, D$_2^{16}$O, HD^{18}O, D$_2^{18}$O HD^{17}O and D$_2^{17}$O. About 38 000 RV transitions were identified using previously known experimental energy levels and accurate variational calculations. A large number, 2880, of precise experimental energy levels are derived for 21 vibrational states of HD^{18}O, D$_2^{18}$O, HD^{17}O and D$_2^{17}$O, about 2000 of them are new. Full results of this study will be published elsewhere [53]. These newly measured data are used in the present analysis for validation, refinement and enlargement of the sets of experimental energy levels provided by the IUPAC project.

4. Results

Table 1 presents a summary of our results in comparison with the 2012 release of HITRAN which contained no data on D$_2$O isotopologues. The data presented for our line lists in the table uses intensity cut-offs suggested for HITRAN 2016 [54] which includes an enhanced cut-off for D$_2$O. The line lists are expected to be essentially complete at 296 K within this constraint. In practice

constructing our line lists required initial consideration of more, generally weaker transitions. Results for each isotopologue are discussed in turn below.

4.1. HD^{16}O

The 2010 IUPAC study [28] derived a set of 8818 consistent experimental energy levels for HD^{16}O based on processing of 54 712 observed RV transitions. Since then a number of studies have recorded HDO spectra using deuterated water samples [55–58]. Very recently accurate measurements of the HD^{16}O line positions and intensities in 100 – 000 and 020 – 000 and 010 – 000 bands have been reported by Devi et al. [59,60]. Weak HDO lines have also been observed in the natural water measurements using high-sensitivity experimental set ups [61–63]. All these new HDO transitions together with earlier validated set [28] were used to enlarge and improve the experimental energy levels set following the MARVEL procedure elaborated in the IUPAC papers. A final set of 9519 accurate HD^{16}O empirical energy levels were derived. Details of this study will be published [64].

The line list computations gave 56 430 transitions between 0 and 19,940 cm^{-1} above the abundance-weighted intensity threshold of 10^{-29} cm/molecule.

Our recommended line list was constructed by replacing the transition wavenumber using the differences between the empirically-determined upper and lower energy levels where possible. As a result, 54 937 line positions out of the total of 56 430 are based on experimental data. A further 1493 transitions whose frequencies were determined using the variational calculations were assigned approximate quantum number label based on the HDO reference list reported by Lavrentieva et al. [22], which leaves only 63 unlabelled transitions. Fig. 1 presents an overview of our new HD^{16}O line list.

The HDO system is characterized by many resonance interactions [65]. 10 476 out of 57 333, or 18% of the lines gave $\rho \geq 1.2$ in our stability analysis. Although many of these transitions are probably still stable, these transitions were assigned HITRAN uncertainty code 3 ($\geq$ 20%).

To check the quality of the line position and intensities, our recommended line list was compared both with original experimental measurements, and with the HITRAN 2012 and GEISA 2015 databases. The ratio between the very recent, accurate experimental transition intensities for the 100 – 000 and 020 – 000 bands in the 2560 – 2850 cm^{-1} spectral region [60] and variational estimates is illustrated on Fig. 2. Very good agreement between the experimental and calculated data is obtained. Defining the root mean square (RMS) average as 100% $\times \frac{(I_{obs} - I_{calc})}{I_{obs}}$ for 200 transitions, our predictions give an RMS of 4.4%, once the 8 worst outliers were excluded. Comparison of the experimental data with the well-known VTT HD^{16}O variational line list [21] and with the HITRAN 2012 database, which used Toth's simulated intensities [66], yields much worse RMSs of 12.4 and 20.2%, respectively.

Fig. 3 presents a similar comparison of this work, HITRAN 2012 and VTT for the 257 high quality measured transition intensities for the 010 - 000 band [59] for which the experimental uncertainty is stated to be $\pm$ 2%. RMSs of 4.1% for this work, 5.3% for VTT, and 6.4% for HITRAN 2012 are obtained after removing 7 outliers. Offsets of respectively about -2 and $+4\%$ from the observed data are obvious for our and the HITRAN 2012 intensities, which are again based on Toth's results [66].

Our HD^{16}O line list contains 56 430 lines and is more than 4 times larger than the 13 237 lines given in the HITRAN 2012 database; this represents an important increase and improvement of the coverage for HD^{16}O over a wide, 0–19,940 cm^{-1}, spectral range, as illustrated by Fig. 1. Line-by-line inter-comparison
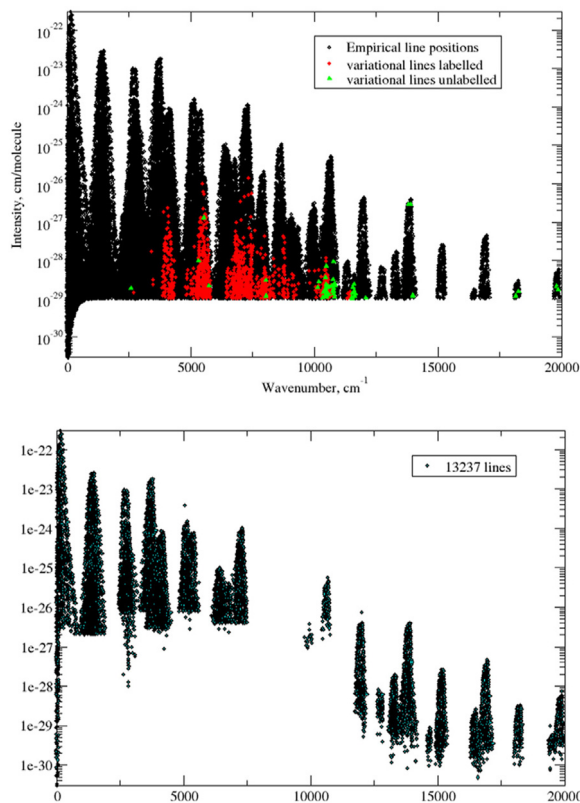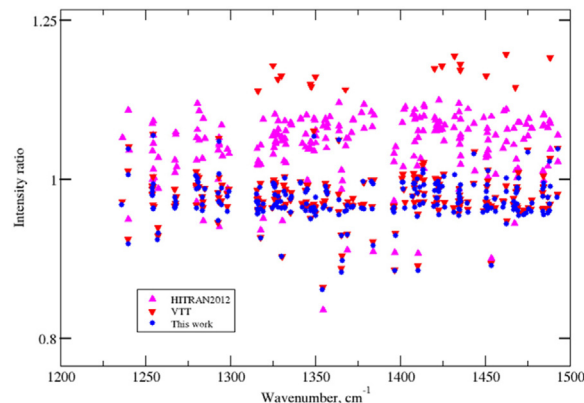
Fig. 1. Composition of our recommended line list for HD^{16}O (upper panel) in comparison with the data lying below 20 000 cm^{-1} provided by HITRAN 2012 (lower panel).
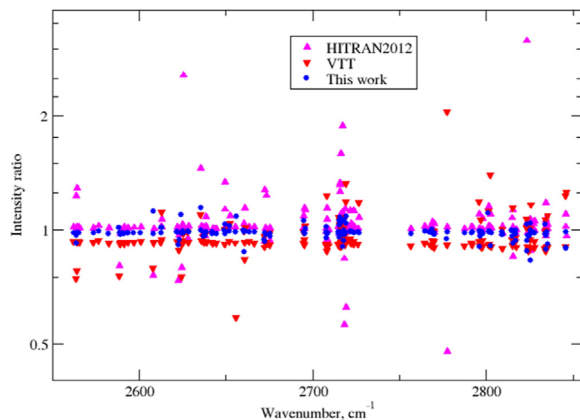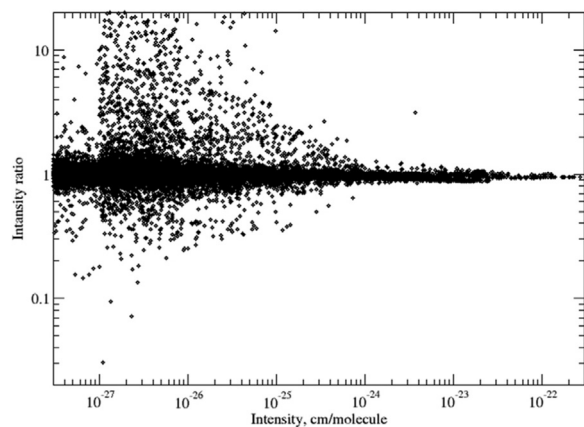

Fig. 2. Ratio of HD^{16}O line intensities at 296 K for various line lists with the accurate measurements of the ν_1 band by Devi et al. [60].

Fig. 3. Ratio of HD^{16}O line intensities at 296 K for various line lists with the accurate measurements of the ν_2 band by Devi et al. [59].

Fig. 4. Comparison between HD^{16}O line lists: ratio of this work to GEISA [16].

reveals large discrepancies both in positions, up to -1.56 cm^{-1}, and, especially prominent, up to 1000% in line intensities between the two line lists. We believe our new line list represents a substantial improvement in both coverage and reliability. However, we note that HITRAN 2012 also contains some data on transitions above 20,000 cm^{-1}.

GEISA 2015 includes an updated set of HD^{16}O transitions, mostly, based on empirical positions, while the intensities largely comprise a mixture of variational VTT [21], and SP [40] data, as well as older measured and simulated values. In total, 53 707 HD^{16}O transitions are given which can be compared to 56 430 in our list. Detailed line-by-line comparison of both databases shows nearly perfect agreement in line positions with just a couple of

dozen outliers. In contrast to line positions, the agreement for intensities is much poorer. The intensity ratio between GEISA and our newly calculated intensities is illustrated in Fig. 4. Large distortions of the intensity ratio up to tens and even hundreds percent were encountered. Inspection of the situation shows that these large discrepancies mostly concern comparison with older GEISA data simulated using an effective Hamiltonian approach.

The variational VTT line list [21] is recognized to be the most accurate variational calculation for HD^{16}O reported so far. It has been used, for example, to study the HDO composition in atmospheres of Earth [67] and other planets [22]. It is therefore useful to compare the intensities given by VTT with those of our new line list. Fig. 5 shows the intensity ratio for HD^{16}O transitions from VTT and those reported here. It can be seen that the intensity ratios are vibrationally dependent. The most prominent disagreements, up to hundreds of percent, are found for the 100 – 000 band which is highlighted on Fig. 5. Some systematic deviations for the strongest intensities were found also for the 010 – 000 and 000 – 000 bands, which are also highlighted. We suggest that these deviations reflect residual problems with the VTT line list.

Finally, Fig. 6 compares a portion of our line list with that given by HITRAN 2012.

4.2. HD^{18}O

Since publication of the IUPAC study [28] in 2010 where validated transitions and energy levels for the HD^{16}O, HD^{18}O, and HD^{17}O were reported, a large number of new data on RV transitions of these molecules have appeared. An update of the IUPAC data will be released soon [64]; below we employ a preliminary
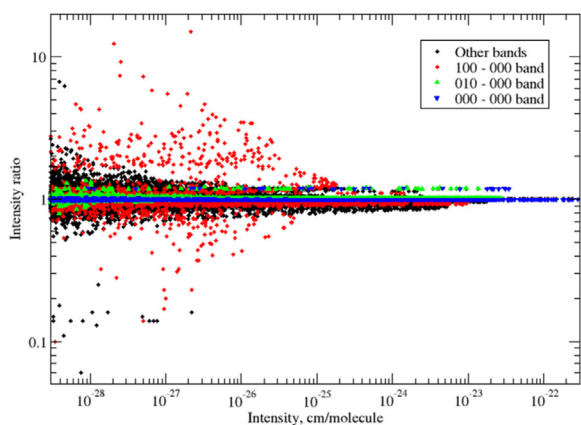
Fig. 5. Comparison between $HD^{16}O$ line lists: ratio of the variational VTT line list [21] to this work.

Table 2
Summary of new experimental data on $HD^{18}O$ rotation-vibration transitions.

Source	Number of lines	Spectral region (cm^{-1})
11LiSoNiHu [68]	1313	989–2148
12LeMiMoKa [62]	8	7151–7304
12MiNaNiVa [55]	5531	6000–9182
12DoTeOrCh [57]	983	6092–6925
13LeMiMoKa [63]	234	6092–6598
12OuReMiTh [69]	923	1069–1863
14LiNaKaCa [56]	1328	5860–6802
16YuPeDrMi [70]	105	15–162
16MiLeKaMo [71]	498	6038–6666
17VaNaScBy [53]	9185	2105–6300

version of these empirical energy levels.

The new data sources used to update the $HD^{18}O$ RV levels beyond those reported in the IUPAC study [28] are given in Table 2. In total, 28 787 transitions, corresponding to 17 262 unique transitions, were validated between 0 and 12,000 cm^{-1}. This should be compared to 8729 (7191 unique) transitions reported for $HD^{18}O$ in the IUPAC study. Fig. 7 illustrates the $HD^{18}O$ transitions whose frequencies could be empirically determined using the previous IUPAC study and by our present study.

A set of 3628 energy levels was derived from the updated set of $HD^{18}O$ transitions following the MARVEL procedure [72,73], while only 1895 energy levels were determined in the IUPAC study [28]. Reasonable vibrational and rotational quantum numbers were assigned to all experimental energy levels based on the extensive

calculations within the effective Hamiltonian (EH) approach [74]. These energy levels combined with line intensities available from recent variational calculations were then used to generate the accurate and detailed "empirical" absorption list of $HD^{18}O$ consisting of about 102 000 lines between 0 and 12,110 cm^{-1} with intensities greater than 10^{-27} cm/molecule for 100% isotopic abundance.

The position accuracy estimate is given for every transition obtained as square root of sum of squared uncertainties of the upper and lower energy level provided by the MARVEL procedure. Details of the EH empirical list construction will be published separately, and can partly be found in Ref. [75].

To prepare the resulting absorption list in HITRAN format, the total variational list was then cut in accordance with the $HD^{18}O$ natural abundance weighted intensity threshold. This gave a set of 10 664 transitions between 0 and 10 730 cm^{-1}. Comparison of this set with the list of empirical transitions allows the variational line positions to be replaced by an empirically derived one for all but
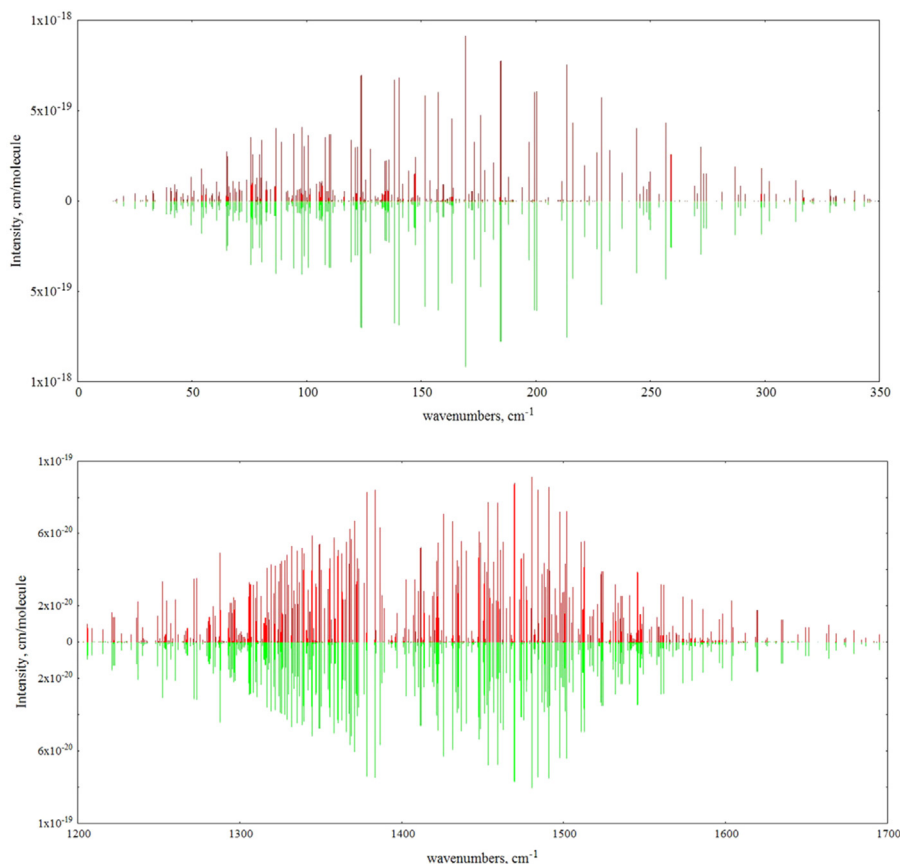
Fig. 6. Comparison of 296 K $HD^{16}O$ spectra given by the current line list (up) with HITRAN 2012 [15] (down). Intensities assume unit abundance for each isotopologue.
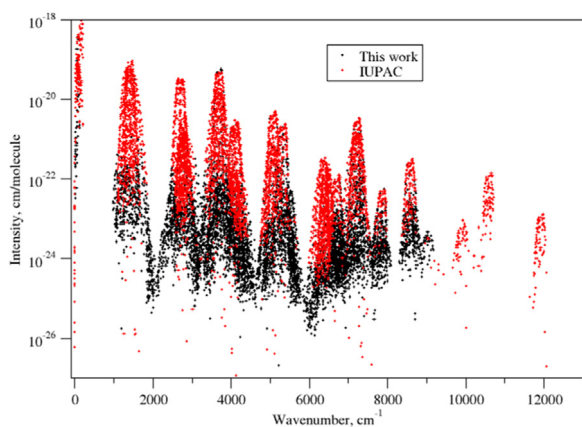
Fig. 7. Comparison between HD^{18}O line lists based on empirically-determined line positions from the IUPAC [28] and the present work.
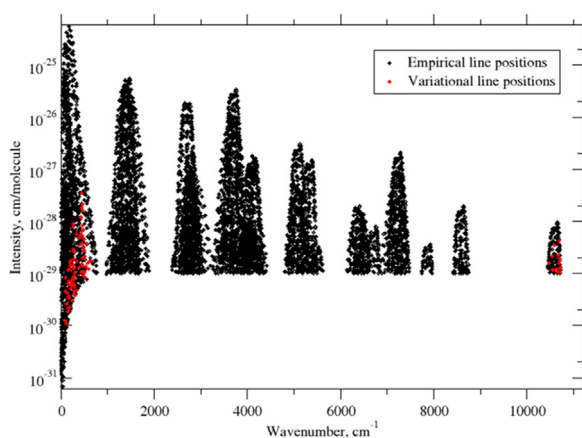

Fig. 8. Composition of our recommended line list for HD^{18}O.

152 transitions which lie between 80–650 and 10,460–10,730 cm^{-1}. Fig. 8 illustrates the number of empirical and pure variational transitions accepted in the resulting list for HD^{18}O molecule.

An RMS deviation between the experimental and variational energy levels was found to be of 0.04 cm^{-1}, while the largest absolute deviation is 0.14 cm^{-1}, as illustrated by Fig. 9. As the pure variational line positions lie inside spectral regions containing the empirically-determined transition frequencies (see Fig. 8), it can be supposed that the accuracy of 152 yet to be observed variational positions is comparable with deviations between variational and observed transitions falling in the same region: about 0.03 and 0.10 cm^{-1} in the 80–650 and 10,460–10730 cm^{-1} spectral regions, respectively.

It is much more difficult to estimate the accuracy of variational intensities used in the resulting list. However, the Lodi-Tennyson procedure [32] allows one to identify unstable calculated intensities. Those intensities which had a scatter factor ρ larger than 2 were deemed as unstable. An analysis of the unstable intensities shows that they are mostly caused by the inaccuracy in the determination of the corresponding wave functions in case of two RV transitions coming on the upper energy levels in close resonance. Then, the inaccuracy of the PES used is responsible for the unstable intensities. As has already been noted [65,76], distortions up to 3 orders of magnitude between the observed and calculated variational intensities can be encountered in cases of intensity borrowing between the strong and weak transition.

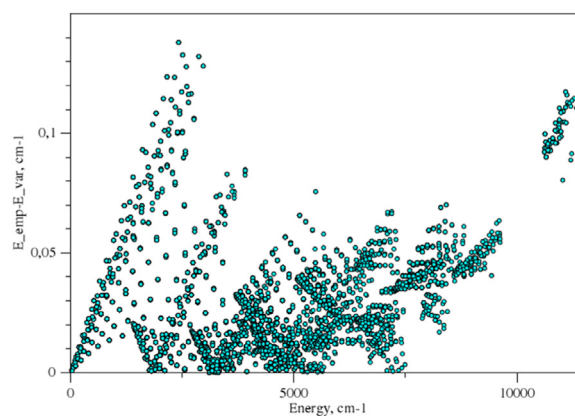For HD^{18}O, only 105 lines (about 1%) of the total 10 664 have

**Fig. 9.** Deviations between the empirical and variational energy levels for HD^{18}O.

$\rho > 2$; a HITRAN accuracy code "4" (10–20%) is assigned for intensities in this case, while the other transition intensities were estimated to be accurate within 2–5% (code "6") which represents a rather cautious choice given the accuracy of typical variational calculations for water performed using a high accuracy DMS [34].

HITRAN 2012 [15] contains only 1611 HD^{18}O transitions which all lie between 0 and 3825 cm^{-1}. Below 333 cm^{-1} these transitions came from the JPL database [77] and involve the 000-000 and 010-010 pure rotational bands. Above 1179 cm^{-1} they came from Toth's empirical SISAM database [66] and comprised the ν_1, ν_2 and ν_3 fundamental bands. Comparison between our list and Toth's data is quite satisfactory: an RMS of only 0.000018 cm^{-1} for line positions and an average intensity ratio of 0.97 for 659 lines.

A more extensive comparison can be made between our HD^{18}O line list and the recent 2015 release of GEISA [16]. The new HD^{18}O line list contained in GEISA 2015 was constructed as follows. The 204 highly accurate experimental microwave and far infrared lines from Johns [78] and Steenbeckeliers, as given by Lovas [79], were used in the 0–200 cm^{-1} region. The positions of the other lines were derived from the experimental energy levels obtained in Refs. [53,55,68,80], while all intensities are given by variationally-calculated values based on Schwenke and Partridge (SP) potential and dipole moment surfaces [25,40] as computed by Tashkun (see www.spectra.iao.ru). In total, GEISA 2015 includes 9760 transitions of HD^{18}O.

The HD^{18}O in GEISA and here are largely empirical lists of frequencies based on the similar sets of energy levels. The agreement between line positions is quite satisfactory with an RMS of 0.001 cm^{-1}, provided that 27 outliers between 0.03 and 0.75 cm^{-1} are excluded. However, the highly accurate line positions from the recent far infrared study of Yu et al. [70] disagree with those adopted in GEISA 2015 by significantly more than the declared uncertainty of $1 \times 10^{-6} – 6 \times 10^{-6}$ cm^{-1}, with an RMS deviation of 0.00018 cm^{-1}. Conversely, the match with our line positions is perfect, see Fig. 10.

As all the HD^{18}O transition intensities in GEISA 2015 database originate from variational calculation of Partridge and Schwenke, then comparison with our values reduces to comparison of two calculated variational data sets. However, as it is obvious from Fig. 11, there are important disagreements between the SP and our calculated intensities for the ν_1 and ν_3 fundamental bands. Most prominent deviations (up to an intensity ratio 1.5) are observed for weak ν_1 lines below 5×10^{-28} cm/molecule. Comparisons with accurate experiments for H$_2$O [34,81,82] suggest that for transitions which are identified as stable, our variational procedure should give intensities within 10% even for troublesome bands.
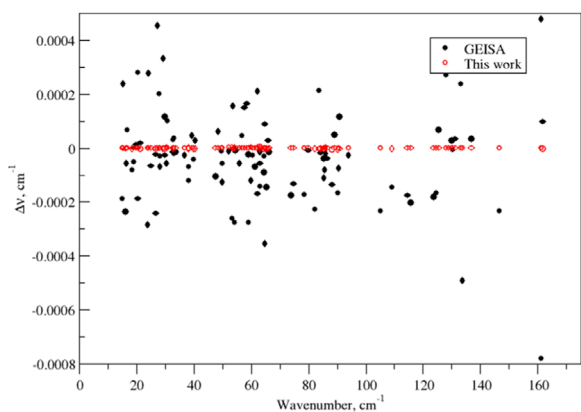
Fig. 10. Comparison between HD^{18}O lines positions measured by Yu et al. [70] and those from this work and GEISA 2015 [16].
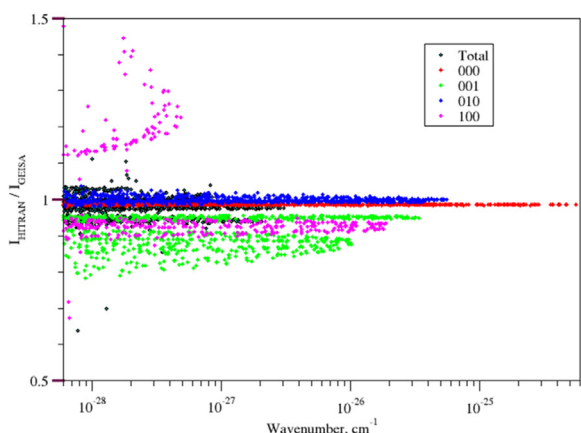
Fig. 11. The intensity ratio between variational intensities for HD^{18}O reported here and those from GEISA 2015 [16].

4.3. HD^{17}O

The HD^{17}O data set validated by the IUPAC study [28] was very limited; it consisted of 483 (442 unique) transitions between 0 and 1674 cm^{-1} belonging to the pure rotational 000-000 band and the ν_2 fundamental band. Our set of HD^{17}O transitions was considerably enlarged by involving the new data from eight sources listed in Table 3. In total, the new set includes 6077 transitions (4933 unique) spanning the 0–8709 cm^{-1} spectral region. A comparison between the previously reported [28] and our newly processed data is shown in Fig. 12. The total number of the energy levels derived is 1620, which is ten times larger than the 162 energy levels for the 000 and 010 vibrational states reported previously. An empirical line list was constructed from the experimental energy levels and intensities provided by the variational calculation in the 0–8899 cm^{-1} spectral region consisting of 46 964 transitions stronger than 10^{-28} cm/molecule for 100% HD^{17}O.

Similar to HD^{18}O, four variational lists were computed and used to identify unstable transitions. These lists were cut in accordance with natural isotopic abundance, and the standard HITRAN 296K intensity threshold. The resulting line list consists of 6366 transitions between 0 and 10 703 cm^{-1}. Inspection of ρ for each transition led to the identification of 69 (1.1%) transitions whose intensities are unstable, for which the HITRAN accuracy codes for the intensities were chosen between "2" and "5" in accordance with the value of ρ. For the majority of transitions the intensity accuracy code "6" i.e. 2–5% is selected.

The frequencies in the best variational line list were changed to

Table 3
Summary of new experimental data on HD^{17}O rotation-vibration transitions.

Source	Number of lines	Spectral region (cm^{-1})
11LiSoNiHu [68]	1661	1113–1929
12PuCaGa [83]	128	2–51
12LeMiMoKa [62]	8	7151–7304
12MiNaNiVa [55]	726	6120–8709
15MeMiTy [84]	184	323–521
14LiNaKaCa [56]	171	6085–6799
16MiLeKaMo [71]	498	6038–6666
17VaNaScBy [53]	2210	2509–6297
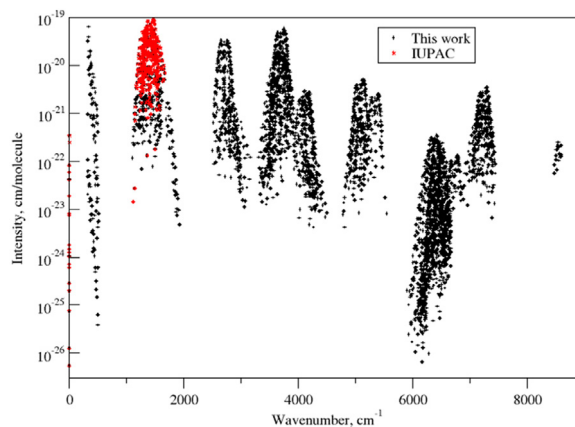
Fig. 12. Comparison between HD^{17}O line lists based on empirically-determined line positions from the IUPAC [28] and the present work.

empirical ones for majority of transitions leaving only 585 transitions with variational positions. The composition of the resulting HD^{17}O list is illustrated on Fig. 13. As for HD^{18}O, the HITRAN accuracy code for empirical position was determined as square root of sum of squared uncertainties of the upper and lower energy level provided by the MARVEL procedure.

The experimental energy levels involved in the final transition list and the variational data show an RMS deviation of 0.054 cm^{-1} and a maximum deviation of 0.21 cm^{-1} for the 1177 energy levels involved. We can then assume that the accuracy of pure variational positions should be no worse than 0.1 cm^{-1} on average and hence give an HITRAN accuracy code "2".

It should be noted that both HITRAN 2012 and GEISA 2015 include only 175 HD^{17}O transitions of the ν_2 band between 1234 and 1599 cm^{-1}, see Fig. 14. These lines agree with our data with RMS of only 0.0002 cm^{-1}, but clearly do not give full coverage for this isotopologue, nor indeed include its most intense transitions.

4.4. D$_2^{16}$O

As there is an enhanced deuterium abundance in various astronomical environments such as the atmosphere of Venus it was decided to consider D$_2$O lines weaker than the standard HITRAN cutoff. The natural abundance-weighted intensity cutoff above 2000 cm^{-1} was reduced to 10^{-32} cm/molecule with proportionate changes at lower wavenumbers. For 100 % D$_2^{16}$O this gives an effective cutoff of 4.13×10^{-25} cm/molecule.

Unlike HDO, the IUPAC study [30] achieved a rather thorough coverage of the D$_2^{16}$O energy levels of interest to us here; in part this is due to the large number of transitions assigned in spectra of hot D$_2$O [85–87].The experimental energy levels reported by Serdyukov et al. [88] were used to improve the variational positions above 10,000 cm^{-1}. As a result it was only necessary to use 200 lines with *ab initio* frequencies out of a total of 23 195 included in
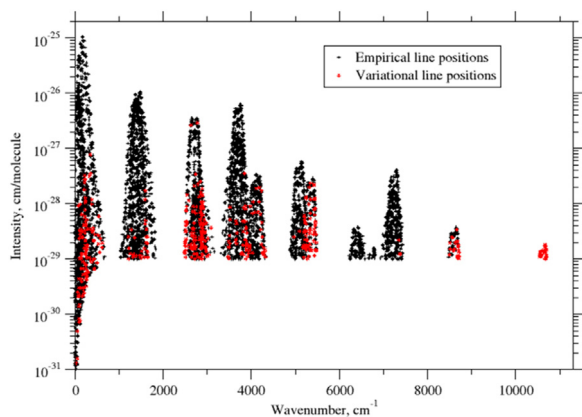
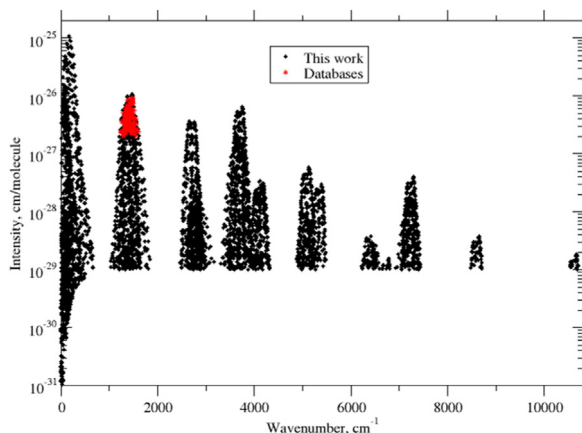**Fig. 13.** Composition of our recommended line list for HD^{17}O.

Fig. 15. Composition of our recommended line list for D$_2^{16}$O.

Fig. 14. Summary of HD^{17}O in the HITRAN 2012 [15] and GEISA 2015 [16] databases, and in the present study.

our final line list. Given the accuracy of the underlying spectro-scopically-determined PES used to generate these lines, we would estimate their predicted frequencies to be accurate to about 0.04 cm^{-1}, giving them a HITRAN uncertainty code of "2". Uncertainties in the other line frequencies were based on the MAR-VEL uncertainties of the upper and lower energy levels. For levels only characterized by hot emission spectra these uncertainties can be relatively large. Fig. 15 presents a summary of our re-commended D$_2^{16}$O line list.

The scatter factor considers all line with $\rho > 1.2$ as less reliable. Since there is no ready data to replace the intensities for these lines, they were retained but given a HITRAN uncertainty code 3 (≥ 20%). We note that use of this low value of ρ is extremely conservative. However, this only gave 1080 unstable lines out of the total 23 915 or about 4.6 %. This low number of even marginally unstable lines is the basis on which it was deemed that the much smaller number, and hence inherently much stronger, lines of D$_2^{17}$O and D$_2^{18}$O are all stable.

4.5. D$_2^{17}$O and D$_2^{18}$O

With the lower intensity cutoff for D$_2$O it is also necessary to consider strong transitions involving D$_2^{17}$O and D$_2^{18}$O. For these species the lowered cut-off translates to 1.08×10^{-21} and 2.01×10^{-22} cm/molecule for 100% D$_2^{17}$O and D$_2^{18}$O, respectively. As can be seen from Table 1, this leads to the retention of a few thousand lines for each isotopologue. As these lines are all intrinsically strong, the issue with large changes in intensity due to resonances does not arise. All these strong lines were assumed to
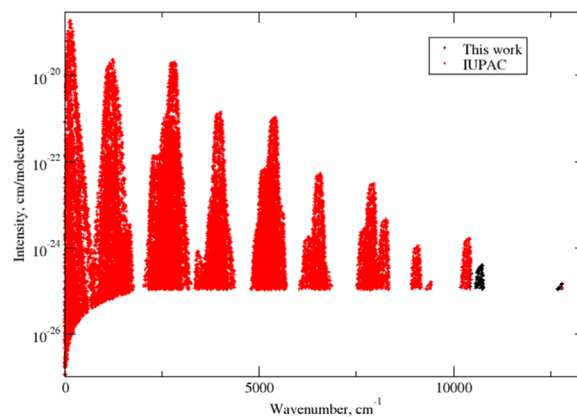
be stable and the results taken from a single line list.

In contrast to D$_2^{16}$O, the number of empirical energy levels re-covered by the IUPAC task group for D$_2^{17}$O and D$_2^{18}$O [30] is com-paratively low. The new experiments that have recently been performed in Hefei [53] on these species result in the assignment of transitions to a large number of previously uncharacterized energy levels. As can be seen from Fig. 16, these new data allow the frequencies of transitions within several new bands to be obtained empirically for the first time.

Use of these new data sources meant that it was possible to get empirical frequencies for a high proportion of the transitions. This meant that for 692 line positions out 2202 for D$_2^{17}$O and 100 out of 3823 for D$_2^{18}$O are estimated from the variational calculations. The predicted frequencies have an estimated accuracy of about 0.04 cm^{-1}, giving them a HITRAN uncertainty code of "2". This figure is in line with the RMS which the calculations reproduce the ob-served transitions for these species. Fig. 16 presents a summary of our recommended line lists for D$_2^{17}$O and D$_2^{18}$O.

4.6. Further comparisons

Recently Mikhailenko et al. [17] presented a detailed database of water isotopologue line positions and intensities covering 5850–8341 cm^{-1}, based on a combination of experimental studies and variational calculations. In this section we compare our re-commendations with theirs.

Overall there is very good agreement in positions between us and Mikhailenko et al.. For HD^{16}O, the empirical line positions reported by them give an RMS difference of only 00077 cm^{-1} compared to ours once 4% of the lines, which are the largest outliers, are excluded. Over half, about 240, of these excluded HD^{16}O line positions appear to originate from unpublished em-pirical lines/energies employed by Mikhailenko et al.. Similar RMSs of 0.00087 and 0.00073 cm^{-1} for HD^{18}O and HD^{17}O lines, respectively.

Of 11,018 HD^{16}O lines given by Mikhailenko et al. [17], experi-mental intensities are provided for 4958 transitions, the other intensity values were based calculations due to Schwenke and Partridge (SP) [40]. These calculations have been well-used but can no longer be regarded as state-of-the-art. The empirical set of intensities includes 1180 values taken from Toth's SISAM database [66] which are based on Fourier transform spectroscopy (FTS) measurements of deuterium-enriched samples between 6131 and 7515 cm^{-1}. A further 3778 transition intensities, for lines between 5895 and 8330 cm^{-1}, were derived from a series of cavity ring-down spectroscopy (CRDS) measurements of natural water [61–63,89,90]. The CRDS HDO transitions are, mostly, weak and very weak, and the measured intensities do not appear to be highly
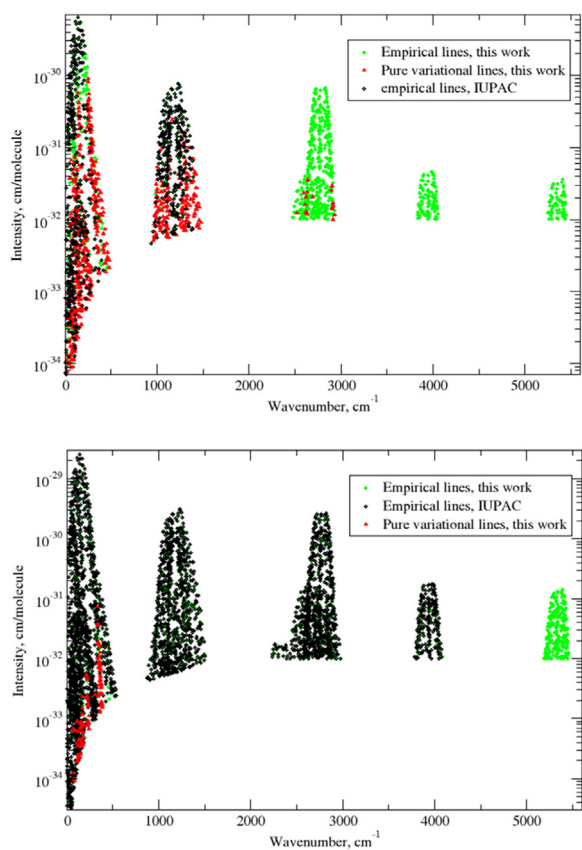
Fig. 17. Ratio of our recommended line intensities for $HD^{16}O$ transitions to the empirical values recommended by Mikhailenko et al.. [17].

Fig. 16. Composition of our recommended line lists for $D_2^{17}O$(upper) and $D_2^{18}O$ (lower).

accurate. Fig. 17 displays the intensity ratio between our recommended intensities and the empirical values included in Mikhailenko et al.'s line list. A RMS of 7.5% is obtained for comparison of our and Toth's intensities once about 7% of the largest outliers are dropped. Our intensities exceed Toth's by about 8%, this is also true for SP [40] and VTT [21] calculated intensities. These difference are in line with comparisons with SISAM data for the main isotopologue [91] which are the main reason that SISAM intensity data is no longer used in HITRAN. Much worse is the comparison with the CRDS intensities; these have an RMS difference of 20% once the 10% largest outliers are removed. As could be anticipated, the comparison between the SP intensities adopted by Mikhailenko et al. our calculated set is much better with RMS of 4.5% for best matched 95% of the 5946 lines we compared. This figure is still larger than our average uncertainty for these lines.

We note the large and erratic dispersions in the intensity ratios between our variational calculations and the CRDS experimental intensities, and note the general agreement between our and previous calculated intensities. We suggest that this problem may be due to insufficiently accuracy of the experimental data rather than issues with the calculations. Experience with use of variational calculations to give accurate intensities has shown that for accurate experimental data and problematic computed intensities the dependence of the I_{obs}/I_{calc} ratio on vibrational and rotational quantum numbers generally behaves in a regular fashion [34]. The HDO line intensities sets reported by Mikhailenko et al.. represent either a mixture of the experimental (including low accuracy) data with SP variational calculated values (their dataset SM_1) or pure variational SP or VTT values dataset (SM_2). We believe that our intensities represent an improvement in accuracy compared to the older SP and VTT simulations. This is confirmed by comparisons with the accurate experimental data performed in this study and
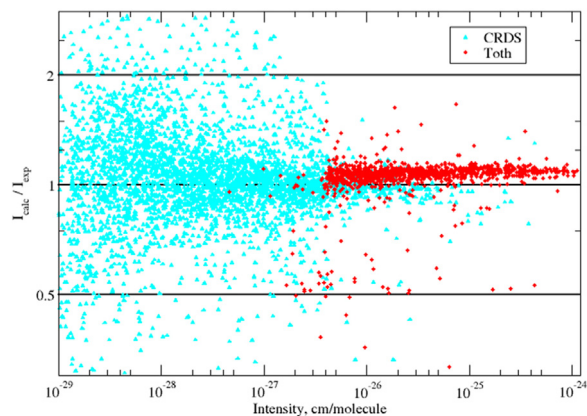
elsewhere [34,39,82]. Our intensities set is also more consistent compared to the mixture of experimental and calculated data proposed by Mikhailenko et al.

5. Conclusion

In this paper we present comprehensive line lists for deuterated isotopologues of water constructed based on the use of frequencies derived from empirically-determined energy levels, where available, and *ab initio* transition intensities. These line lists have the virtue of being complete for the intensity cutoffs specified at 296 K. We also believe that in nearly all cases they represent the best available data for these isotopologues; the exception being the cases where there are direct, high accuracy measurements of individual lines. We therefore recommend that these line lists be used as the basis of deuterated water data in future releases of atmospheric databases.

Of course the process of constructing line lists is one of continuous improvement. Work on improving and extending the list of empirical energy levels for water using the MARVEL procedure is ongoing [64]. Furthermore, recent comparisons with high quality experiments for H_2O [34] have suggested areas where the *ab initio* intensity predictions should be further improved. Work in this direction is currently underway. Finally, improvements in the model, and in particular the potential energy surface, used to compute vibration-rotation wave functions will reduce problems with unstable transition intensities are due poorly treated resonance interactions; this will allow a greater proportion of the transition intensities to be computed reliably *ab initio*.

This work, when combined with the previous study by Lodi and Tennyson [32] on $H_2^{17}O$ and $H_2^{18}O$ means that hybrid, HITRAN-style line lists are now available for all the minor isotopologues of water. Some work in this direction has been performed on $H_2^{16}O$ [34] but this will be the subject of further study.

Supplementary material

Supplementary material associated with this article can be found, in the online version, at http://dx.doi.org/10.1016/j.jqsrt.2017.06.026

References

[1] Joussaume S, Sadourny R, Jouzel J. A general-circulation model of water isotope cycles in the atmosphere. Nature 1984;311:24–9. http://dx.doi.org/10.1038/311024a0.

[2] Ridal M, Jonsson A, Werner M, Murtagh DP. A one-dimensional simulation of the water vapor isotope HDO in the tropical stratosphere. J Geophys Res 2001;106:32283–94. http://dx.doi.org/10.1029/2000JD000268.

[3] Schmidt GA, Hoffmann G, Shindell DT, Hu YY. Modeling atmospheric stable water isotopes and the potential for constraining cloud processes and stratosphere-troposphere water exchange. J Geophys Res 2005;110:D21314. http://dx.doi.org/10.1029/2005JD005790.

[4] Frankenberg C, Yoshimura K, Warneke T, Aben I, Butz A, Deutscher N, et al. Dynamic processes governing lower-tropospheric HDO/H2O ratios as observed from space and ground. Science 2009;325:1374–7. http://dx.doi.org/10.1126/science.1173791.

[5] Yoshimura K, Frankenberg C, Lee J, Kanamitsu M, Worden J, Rockmann T. Comparison of an isotopic atmospheric general circulation model with new quasi-global satellite measurements of water vapor isotopologues. J Geophys Res 2011;116:D19118. http://dx.doi.org/10.1029/2011JD016035.

[6] Zhang X, Zhang X, Guan H, Huang Y, Wu H. Spatiotemporal distributions of delta d in atmospheric water vapor based on TES data during 2004–2009. Acta Meteorologica Sinica 2012;26:683–99. http://dx.doi.org/10.1007/s13351-012-0602-5.

[7] Boesch H, Deutscher NM, Warneke T, Byckling K, Cogan AJ, Griffith DWT, et al. HDO/H2O ratio retrievals from GOSAT. Atmos Meas Tech 2013;6:599–612. http://dx.doi.org/10.5194/amt-6-599-2013.

[8] Yoshimura K. Stable water isotopes in climatology, meteorology, and hydrology: a review. J Met Soc Japan 2015;93:513–33. http://dx.doi.org/10.2151/jmsj.2015-036.

[9] Werner M, Haese B, Xu X, Zhang X, Butzin M, Lohmann G. Glacial-interglacial changes in (H2O)-o-18, HDO and deuterium excess - results from the fully coupled ECHAM5/MPI-OM earth system model. Geosci Model Dev 2016;9:647–70. http://dx.doi.org/10.5194/gmd-9-647-2016.

[10] Fouchet T, Lellouch E. Vapor pressure isotope fractionation effects in planetary atmospheres: application to deuterium. Icarus 2000;144:114–23. http://dx.doi.org/10.1006/icar.1999.6264.

[11] Montmessin F, Fouchet T, Forget F. Modeling the annual cycle of HDO in the martian atmosphere. J Geophys Res 2005;110:E03006. http://dx.doi.org/10.1029/2004JE002357.

[12] De Bergh C, Bezard B, Owen T, Crisp D, Maillard J-P, Lutz BL. Deuterium on Venus - observations from Earth. Science 1991;251:547–9. http://dx.doi.org/10.1126/science.251.4993.547.

[13] Bockelee-Morvan D, Gautier D, Lis DC, Young K, Keene J, Phillips T, et al. Deuterated water in comet c 1996 b2 (hyakutake) and its implications for the origin of comets. Icarus 1998;133:147–62. http://dx.doi.org/10.1006/icar.1998.5916.

[14] Villanueva GL, Mumma MJ, Bonev BP, Novak RE, Barber RJ, DiSanti MA. Water in planetary and cometary atmospheres: H2O/HDO transmittance and fluorescence models. J Quant Spectrosc Radiat Transf 2012;113:202–20. http://dx.doi.org/10.1016/j.jqsrt.2011.11.001.

[15] Rothman LS, Gordon IE, Babikov Y, Barbe A, Benner DC, Bernath PF, et al. The HITRAN 2012 molecular spectroscopic database. J Quant Spectrosc Radiat Transf 2013;130:4–50. http://dx.doi.org/10.1016/j.jqsrt.2013.07.002.

[16] Jacquinet-Husson N, Armante R, Scott NA, Chédin A, Crépeau L, Boutammine C, et al. The 2015 edition of the GEISA spectroscopic database. J Mol Spectrosc 2016;327:31–72. http://dx.doi.org/10.1016/j.jms.2016.06.007.

[17] Mikhailenko SN, Kassi S, Mondelain D, Gamache RR, Campargue A. A spectroscopic database for water vapor between 5850 and 8340 cm^{-1}. J Quant Spectrosc Radiat Transf 2016;179:198–216. http://dx.doi.org/10.1016/j.jqsrt.2016.03.035.

[18] Coutens A, Jorgensen JK, Persson MV, van Dishoeck EF, Vastel C, Taquet V. High D2O/HDO ratio in the inner regions of the low-mass protostar NGC 1333 IRAS2A. Astrophys J Lett 2014;792:L5. http://dx.doi.org/10.1088/2041-8205/792/1/L5.

[19] Butner HM, Charnley SB, Ceccarelli C, Rodgers SD, Pardo JR, Parise B, et al. Discovery of interstellar heavy water. Astrophys J 2007;659:L137–40. http://dx.doi.org/10.1086/517883.

[20] Bockelee-Morvan D. Private communication. 2017.

[21] Voronin BA, Tennyson J, Tolchenov RN, Lugovskoy AA, Yurchenko SN. A high accuracy computed line list for the HDO molecule. Mon Not R Astron Soc 2010;402:492–6.

[22] Lavrentieva NN, Voronin BA, Naumenko OV, Bykov AD, Fedorova AA. Linelist of HD^{16}O for study of atmosphere of terrestrial planets (Earth, Venus and Mars). Icarus 2014;236:38–47.

[23] Shirin SV, Zobov NF, Polyansky OL, Tennyson J, Parekunnel T, Bernath PF.

[24] Shirin SV, Zobov NF, Polyansky OL. Theoretical line list of D$_2^{16}$O up to 16,000 cm^{-1} with an accuracy close to experimental. J Quant Spectrosc Radiat Transf 2008;109:549–58. http://dx.doi.org/10.1016/j.jqsrt.2007.07.010.

[25] Partridge H, Schwenke DW. The determination of an accurate isotope dependent potential energy surface for water from extensive ab initio calculations and experimental data. J Chem Phys 1997;106:4618–39. http://dx.doi.org/10.1063/1.473987.

[26] Gamache RR, Farese M, Renaud CL. A spectral line list for water isotopologues in the 1100–4100 cm^{-1} region for application to CO$_2$-rich planetary atmospheres. J Mol Spectrosc 2016;326:144–50. http://dx.doi.org/10.1016/j.jms.2015.09.001.

[27] Tennyson J, Bernath PF, Brown LR, Campargue A, Carleer MR, Császár AG, et al. IUPAC critical evaluation of the rotational-vibrational spectra of water vapor. Part I. Energy levels and transition wavenumbers for H$_2^{17}$O and H$_2^{18}$O. J Quant Spectrosc Radiat Transf 2009;110:573–96. http://dx.doi.org/10.1016/j.jqsrt.2009.02.014.

[28] Tennyson J, Bernath PF, Brown LR, Campargue A, Carleer MR, Császár AG, et al. IUPAC critical evaluation of the rotational-vibrational spectra of water vapor. part II. energy levels and transition wavenumbers for HD^{16}O, HD^{17}O, and HD^{18}O. J Quant Spectrosc Radiat Transf 2010;111:2160–84. http://dx.doi.org/10.1016/j.jqsrt.2010.06.012.

[29] Tennyson J, Bernath PF, Brown LR, Campargue A, Carleer MR, Császár AG, et al. IUPAC critical evaluation of the rotational-vibrational spectra of water vapor. part III. energy levels and transition wavenumbers for H$_2^{16}$O. J Quant Spectrosc Radiat Transf 2013;117:29–80. http://dx.doi.org/10.1016/j.jqsrt.2012.10.002.

[30] Tennyson J, Bernath PF, Brown LR, Campargue A, Császár AG, Daumont L, et al. IUPAC critical evaluation of the rotational-vibrational spectra of water vapor. part IV. energy levels and transition wavenumbers for D$_2^{16}$O, D$_2^{17}$O and D$_2^{18}$O. J Quant Spectrosc Radiat Transf 2014;142:93–108. http://dx.doi.org/10.1016/j.jqsrt.2014.03.019.

[31] Tennyson J, Bernath PF, Brown LR, Campargue A, Császár AG, Daumont L, et al. A database of water transitions from experiment and theory (IUPAC technical report). Pure Appl Chem 2014;86:71–83. http://dx.doi.org/10.1515/pac-2014-5012.

[32] Lodi L, Tennyson J. Line lists for H$_2^{18}$O and H$_2^{17}$O based on empirically-adjusted line positions and ab initio intensities. J Quant Spectrosc Radiat Transf 2012;113:850–8. http://dx.doi.org/10.1016/j.jqsrt.2012.02.023.

[33] Regalia L, Oudot C, Mikhailenko S, Wang L, Thomas X, Jenouvrier A, et al. Water vapor line parameters from 6450 to 9400 cm^{-1}. J Quant Spectrosc Radiat Transf 2014;136:119–36. http://dx.doi.org/10.1016/j.jqsrt.2013.11.019.

[34] Birk M, Wagner G, Loos J, Lodi L, Polyansky OL, Kyuberis AA, et al. Accurate line intensities for water transitions in the infrared: comparison of theory and experiment. J Quant Spectrosc Radiat Transf. doi:http://dx.doi.org/10.1016/j.jqsrt.2017.03.040.

[35] Zak E, Tennyson J, Polyansky OL, Lodi L, Tashkun SA, Perevalov VI. A room temperature CO$_2$ line list with ab initio computed intensities. J Quant Spectrosc Radiat Transf 2016;177:31–42. http://dx.doi.org/10.1016/j.jqsrt.2015.12.022.

[36] Zak EJ, Tennyson J, Polyansky OL, Lodi L, Zobov NF, Tashkun SA, et al. Room temperature line lists for CO$_2$ symmetric isotopologues with ab initio computed intensities. J Quant Spectrosc Radiat Transf 2017;189:267–80. http://dx.doi.org/10.1016/j.jqsrt.2016.11.022.

[37] Zak EJ, Tennyson J, Polyansky OL, Lodi L, Zobov NF, Tashkun SA, et al. Room temperature line lists for CO$_2$ asymmetric isotopologues with ab initio computed intensities. J Quant Spectrosc Radiat Transf 2017. http://dx.doi.org/10.1016/j.jqsrt.2017.01.037. In press.

[38] Bernath PF. Spectra of Atoms and Molecules. 2nd edition. Oxford University Press; 2005.

[39] Lodi L, Tennyson J, Polyansky OL. A global, high accuracy ab initio dipole moment surface for the electronic ground state of the water molecule. J Chem Phys 2011;135:034113. http://dx.doi.org/10.1063/1.3604934.

[40] Schwenke DW, Partridge H. Convergence testing of the analytic representation of an ab initio dipole moment function for water: improved fitting yields improved intensities. J Chem Phys 2000;113:6592–7.

[41] Tennyson J. Vibration-rotation transition intensities from first principles. J Mol Spectrosc 2014;298:1–6. http://dx.doi.org/10.1016/j.jms.2014.01.012.

[42] Assafrao D, Mohallem JR. The isotopic dipole moment of HDO. J Phys B 2007;40:F85–91. http://dx.doi.org/10.1088/0953-4075/40/5/F02.

[43] Hobson SL, Valeev EF, Csaszar AG, Stanton JF. Is the adiabatic approximation sufficient to account for the post-born-oppenheimer effects on molecular electric dipole moments? Mol Phys 2009;107:1153–9. http://dx.doi.org/10.1080/00268970902780262.

[44] Tennyson J, Kostin MA, Barletta P, Harris GJ, Polyansky OL, Ramanlal J, et al. DVR3D: a program suite for the calculation of rotation-vibration spectra of triatomic molecules. Comput Phys Commun 2004;163:85–116.

[45] Down MJ. PhD Thesis, Assignment of trace atmospheric species.London, UK: University College London; 2014.

[46] Yurchenko SN, Voronin BA, Tolchenov RN, Doss N, Naumenko OV, Thiel W, et al. Potential energy surface of HDO up to 25000 cm^{-1}. J Chem Phys 2008;128:044312.

[47] Barletta P, Shirin SV, Zobov NF, Polyansky OL, Tennyson J, Valeev EF, et al. CVRQD Adiabatic ab initio ground-state potential surfaces for the water molecule. J Chem Phys 2006;125:204307.

Analysis of hot D$_2$O emission using spectroscopically-determined potentials. J Chem Phys 2004;120:206–10.

[48] Galvao BRL, Rodrigues SPJ, Varandas AJC. Energy-switching potential energy surface for the water molecule revisited: a highly accurate singled-sheeted form. J Chem Phys 2008;129:044302.

[49] Boyarkin OV, Koshelev M, Makarev D, Zobov NF, Polyansky OL. 2017. (to be published).

[50] Lampel J, Pöhler D, Polyansky OL, Kyuberis AA, Zobov NF, Tennyson J, et al. Detection of water vapour absorption around 363 nm in measured atmospheric absorption spectra and its effect on DOAS evaluations. Atmos Chem Phys 2017;17:1271–95. http://dx.doi.org/10.5194/acp-2016-388.

[51] Polyansky OL, Kyuberis AA, Lodi L, Tennyson J, Ovsyannikov RI, Zobov NF, et al. Exomol molecular line lists XXIII: a complete high-accuracy line list for water. Mon Not R Astron Soc.

[52] Ni H-Y, Liu A-W, Song K-F, Hu S-M, Naumenko O, Kruglova T, et al. High-resolution spectroscopy of the triple-substituted isotopologue of water molecule D$_2^{18}$O: the first triad. Mol Phys 2008;106:1793.

[53] Vasilenko IA, Naumenko OV, Scherbakov AP, Bykov AD, Liu A-W, Hu S-M. Fourier transform absorption spectrum of deuterated water vapor enriched by ^{18}O between 2088 and 4600 cm^{-1}. J Quant Spectrosc Radiat Transf 2017. (submitted)

[54] Gordon IE, et al. The HITRAN 2016 molecular spectroscopic database. J Quant Spectrosc Radiat Transf. 2017.

[55] Mikhailenko SN, Naumenko OV, Nikitin AV, Vasilenko IA, Liu A-W, Song K-F, et al. Absorption spectrum of deuterated water vapor enriched by ^{18}O between 6000 and 9200 cm^{-1}. J Quant Spectrosc Radiat Transf 2012;113:653–69.

[56] Liu AW, Naumenko V, Kassi S, Campargue A. CW-cavity ring down spectroscopy of deuterated water in the 1.58 μm atmospheric transparency window. J Quant Spectrosc Radiat Transf 2014;138:97–106. http://dx.doi.org/10.1016/j.jqsrt.2014.02.002.

[57] Down MJ, Tennyson J, Orphal J, Chelin P, Ruth AA. Analysis of an ^{18}O and D enhanced water spectrum AND new assignments for the rare HD^{18}O and HD^{16}O. J Mol Spectrosc 2012;282:1–8.

[58] Daumont L, Jenouvrier A, Mikhailenko S, Carleer M, Hermans C, Fally S, et al. High resolution fourier transform spectroscopy of HD^{16}O: line positions, absolute intensities and self broadening coefficients in the 8800-11,600 cm^{-1} spectral region. J Quant Spectrosc Radiat Transf 2012;113:878–88.

[59] Devi VM, Benner DC, Sung K, Crawford TJ, Gamache RR, Renaud CL, et al. Line parameters for CO$_2$- and self-broadening in the ν_2 band of HD^{16}O. J Quant Spectrosc Radiat Transf 2017;187:472–88. http://dx.doi.org/10.1016/j.jqsrt.2016.10.004.

[60] Devi VM, Benner DC, Sung K, Crawford TJ, Gamache RR, Renaud CL, et al. Line parameters for CO$_2$- and self-broadening in the ν_1 band of HD^{16}O. J Quant Spectrosc Radiat Transf 2017. http://dx.doi.org/10.1016/j.jqsrt.2017.01.032.

[61] Mikhailenko S, Kassi S, Wang L, Campargue A. The absorption spectrum of water in the 1.25 μm transparency window (7408 – 7920 cm^{-1}). J Mol Spectrosc 2011;269:92–103.

[62] Leshchishina O, Mikhailenko S, Mondelain D, Kassi S, Campargue A. CRDS of water vapor at 0.1 torr between 6886 and 7406 cm^{-1}. J Quant Spectrosc Radiat Transf 2012;113:2155–66.

[63] Leshchishina O, Mikhailenko S, Mondelain D, Kassi S, Campargue A. An improved line list for water vapor in the 1.5 μm transparency window by highly sensitive CRDS between 5852 and 6607 cm^{-1}. J Quant Spectrosc Radiat Transf 2013;130:69–80.

[64] Furtenbacher T, Dénes N, Tennyson J, Naumenko OV, Polyansky OL, Zobov NF, et al. The 2016 update of the IUPAC database of water energy levels. J Quant Spectrosc Radiat Transf (in preparation).

[65] Voronin BA, Naumenko OV, Carleer M, Coheur P-F, Fally S, Jenouvrier A, et al. HDO absorption spectrum above 11500 cm^{-1}: assignment and dynamics. J Mol Spectrosc 2007;244:87–101.

[66] Toth RA. SISAM database. 2007. http://mark4sun.jpl.nasa.gov.

[67] Chesnokova TY, Voronin BA, Bykov AD, Zhuravleva TB, Kozodoev AV, Lugovskoy AA, et al. Calculation of solar radiation atmospheric absorption with different H$_2$O spectral line data banks. J Mol Spectrosc 2009;256:41–4.

[68] Liu A-W, Song K-F, Ni H-Y, Hu S-M, Naumenko OV, Vasilenko IA, et al. (0 0 0) And (0 1 0) energy levels of the HD^{18}o and image molecules from analysis of their ν_2 bands. J Mol Spectrosc 2011;265:26–38.

[69] Oudot C, Régalia L, Mikhailenko S, Thomas X, Von Der Heyden DP, Décatoire D. Fourier transform measurements of H$_2^{18}$O and HD^{18}O in the spectral range 1000-2300 cm^{-1}. J Quant Spectrosc Radiat Transf 2012;113:859–69.

[70] Yu S, Pearson JC, Drouin BJ, Miller CE, Kobayashi K, Matsushima F. Terahertz spectroscopy of ground state (HDO)-o-18. J Mol Spectrosc 2016;328:27–31. http://dx.doi.org/10.1016/j.jms.2016.07.005.

[71] Mikhailenko SN, Leshchishina O, Karlovets EV, Mondelain D, Kassi S, Campargue. A. CRDS of ^{17}O enriched water between 5850 and 6671 cm^{-1}: more than 1000 energy levels of H$_2^{17}$O and HD^{17}O newly determined. J Quant Spectrosc Radiat Transf 2016;177:108–16.

[72] Furtenbacher T, Császár AG, Tennyson J. MARVEL: measured active rotational-vibrational energy levels. J Mol Spectrosc 2007;245:115–25.

[73] Furtenbacher T, Császár AG. MARVEL: measured active rotational-vibrational energy levels. II. algorithmic improvements. J Quant Spectrosc Radiat Transf 2012;113:929–35.

[74] Vasilenko IA, Naumenko OV, Kalinin KV, Bykov AD. Simulation of the vibrational-rotational energy levels of D$_2^{18}$O, HD^{18}O, D$_2^{17}$O, and HD^{17}O molecules by the effective hamiltonian approach. Atmos Oceanic Optics 2015;29:216–24.

[75] Vasilenko IA, Naumenko OV. Empirical absorption linelists of the HD^{18}O D$_2^{18}$O molecules. Atmos Oceanic Optics 2015;28:607–13.

[76] Campargue A, Vasilenko I, Naumenko O. Intracavity laser absorption spectroscopy of HDO between 11 645 and 12 330 cm^{-1}. J Mol Spectrosc 2005;234:216–27. http://dx.doi.org/10.1016/j.jms.2005.09.007.

[77] Pickett HM, Poynter RL, Cohen EA, Delitsky ML, Pearson JC, Müller HSP. Submillimeter, millimeter, and microwave spectral line catalog. J Quant Spectrosc Radiat Transf 1998;60:883–90.

[78] Johns JWC. High-resolution far-infrared (20-350-cm^{-1}) spectra of several isotopic species of H$_2$O. J Opt Soc Am B 1985;2:1340–54.

[79] Lovas FJ. Microwave spectral tables. II. Triatomic molecules. J Phys Chem Ref Data 1978;7:1445–750.

[80] Liu AW, Du JH, Song KF, Wang L, Wan L, Hu SM. High-resolution fourier-transform spectroscopy of ^{18}O-enriched water molecule in the 1080–7800 cm^{-1} region. J Mol Spectrosc 2006;237:149–62.

[81] Hodges JT, Lisak D, Lavrentieva N, Bykov A, Sinitsa L, Tennyson J, et al. Comparison between theoretical calculations and high-resolution measurements of pressure-broadening for water vapor spectra near 935 nm. J Mol Spectrosc 2008;249:86–94.

[82] Grechko M, Aseev O, Rizzo TR, Zobov NF, Lodi L, Tennyson J, et al. Stark coefficients for highly excited rovibrational states of H$_2$O. J Chem Phys 2012;136:244308.

[83] Puzzarini C, Cazzoli G, Gauss J. The rotational spectra of HD^{17}O and D$_2^{17}$O: Experiment and quantumchemical calculations. J Chem Phys 2012;137:154311. http://dx.doi.org/10.1063/1.4758316.

[84] Mellau GC, Mikhailenko SN, Tyuterev VG. Hot water emission spectra: rotational energy levels of the (000) and (010) states of (HDO)-o-17. J Mol Spectrosc 2015;308:6–19. http://dx.doi.org/10.1016/j.jms.2014.12.023.

[85] Mellau G, Mikhailenko SN, Starikova EN, Tashkun SA, Over H, Tyuterev VG. Rotational levels of the (000) and (010) states of D$_2^{16}$O from hot emission spectra in the 320–860 cm^{-1} region. J Mol Spectrosc 2004;224:32–60.

[86] Mikhailenko SN, Mellau GC, Starikova EN, Tashkun SA, Tyuterev VG. Analysis of the first triad of interacting states (020), (100), and (001) of D$_2^{16}$O from hot emission spectra. J Mol Spectrosc 2005;233:32–59.

[87] Zobov NF, Ovsannikov RI, Shirin SV, Polyansky OL, Tennyson J, Janka A, et al. Infrared emission spectrum of hot D$_2$O. J Mol Spectrosc 2006;240:112–9.

[88] Serdyukov VI, Sinitsa LN, Bykov AD, Polovtseva ER, Scherbakov AP. Absorption spectrum of D$_2$O between 10000–11000 cm^{-1}. J Quant Spectrosc Radiat Transf 2017. http://dx.doi.org/10.1016/j.jqsrt.2017.02.009.

[89] Macko P, Romanini D, Mikhailenko SN, Naumenko OV, Kassi S, Jenouvrier A, et al. High sensitivity CW-cavity ring down spectroscopy of water in the region of the 1.5 μm atmospheric window. J Mol Spectrosc 2004;227:90–108.

[90] Campargue A, Mikhailenko SN, Lohan BG, Karlovets EV, Mondelain D, Kassi S. The absorption spectrum of water vapor in the 1.25 mu m atmospheric window (7911–8337 cm(-1)). J Quant Spectrosc Radiat Transf 2015;157:135–52. http://dx.doi.org/10.1016/j.jqsrt.2015.02.011.

[91] Tolchenov RN, Tennyson J. Water line parameters for weak lines in the range 7400–9600 cm^{-1}. J Mol Spectrosc 2005;231:23–7.